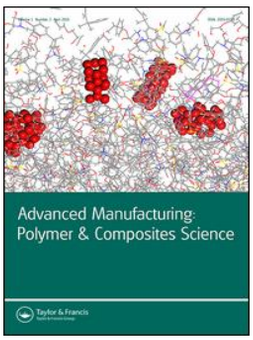

Taylor & Francis
Taylor & Francis Group

Advanced Manufacturing: Polymer & Composites Science

ISSN: 2055-0340 (Print) 2055-0359 (Online) Journal homepage: https://www.tandfonline.com/loi/yadm20

Design and application of discontinuous resin distribution patterns for semi-pregs

Sarah G. K. Schechter, Lessa K. Grunenfelder & Steven R. Nutt

To cite this article: Sarah G. K. Schechter, Lessa K. Grunenfelder & Steven R. Nutt (2020): Design and application of discontinuous resin distribution patterns for semi-pregs, Advanced Manufacturing: Polymer & Composites Science, DOI: 10.1080/20550340.2020.1736864

To link to this article: https://doi.org/10.1080/20550340.2020.1736864

Published online: 07 Apr 2020.

ADVANCED MANUFACTURING: POLYMER & COMPOSITES SCIENCE
https://doi.org/10.1080/20550340.2020.1736864

Design and application of discontinuous resin distribution patterns for semi-pregs

Sarah G. K. Schechter, Lessa K. Grunenfelder and Steven R. Nutt

Department of Chemical Engineering and Materials Science, University of Southern California, Los Angeles, California, USA

ABSTRACT

Vacuum-bag-only (VBO) prepregs fabricated with discontinuous resin (semi-pregs) on a unidirectional fiber bed reportedly exhibit high through-thickness permeability and yield high-quality laminates, even under adverse process conditions, such as poor vacuum or long out-times. In this work, semi-pregs were fabricated using fiber beds of various weaves, fiber types, and areal weights (200–670 GSM). Flat and curved laminates were produced and characterized, confirming that porosity-free parts can be manufactured from a range of constituent materials using VBO semi-pregs. Contoured laminates were produced with negligible porosity, although a slight increase in bulk factor of prepreg plies was observed ($\Delta \sim 0.1$). In addition, design considerations and limitations for the fabrication of semi-pregs were presented. The findings demonstrate that polymer film dewetting can be used effectively to produce semi-pregs that yield porosity-free laminates *via* VBO processing, imparting robustness to out-of-autoclave cure of prepreg laminates.

KEYWORDS

Prepreg; polymer matrix composites; porosity; defects; out of autoclave; vacuum bag only

GRAPHICAL ABSTRACT

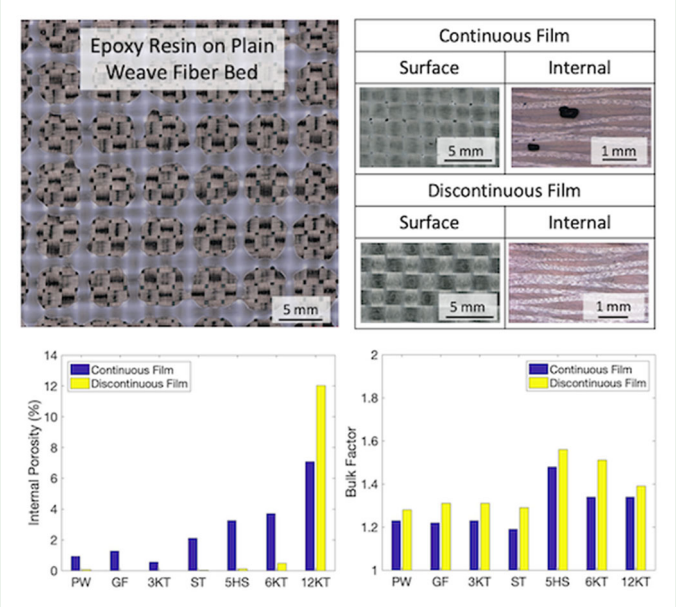

1. Introduction

The application of discontinuous resin on different fibers beds was evaluated for use in commonly encountered manufacturing conditions for out-of-autoclave (OoA)/vacuum-bag-only (VBO) processing of composite prepregs, and design considerations were determined for the fabrication of such prepregs. The study was motivated by limitations of current methods for producing composite parts for aerospace, which are commonly cured in high-pressure autoclaves (heated pressure vessels). These methods consistently yield defect-free parts, but autoclave processing has drawbacks, including high capital and operational cost, size restrictions, limited throughput (production bottlenecks), and high resource use (e.g. energy, nitrogen gas). Alternative manufacturing methods are sought to

CONTACT Sarah G. K. Schechter sarahgka@usc.edu Department of Chemical Engineering and Materials Science, University of Southern California, Los Angeles, CA, USA

reduce costs, overcome limitations, and accelerate production rates, particularly in aerospace [1].

VBO processing of composites offers a viable alternative to conventional autoclave cure methods [2, 3]. VBO processing is an OoA method in which prepreg is vacuum bagged and cured in an oven. VBO processed parts can match the quality of parts manufactured in an autoclave under favorable conditions. However, adverse process conditions, including poor vacuum, incomplete air evacuation, and/or high humidity, often yield defects, particularly porosity, which degrade mechanical performance [4]. For every percent of void content in a composite, up to a total void content of ∼4%, the interlaminar shear strength decreases ∼7%, regardless of the resin, fiber type, or fiber surface treatment [5]. Because VBO processing is limited to a consolidation pressure of 0.1 MPa (1 atm), air and other gases can be trapped during layup. Once the resin gels, trapped bubbles remain, resulting in potentially unacceptable porosity levels (>1%). For VBO processing to gain wider acceptance in high-performance applications, the process must consistently yield low porosity levels.

Background. Previous work has shown that use of OoA/VBO prepregs with a discontinuous resin pattern (semi-pregs) virtually eliminates porosity caused by entrapped air or moisture, without an autoclave cure [6]. For example, Grunenfelder [7–9] showed that even under adverse process conditions, parts cured using semi-preg contained near-zero internal porosity and no surface defects. In contrast, conventional VBO prepreg (with continuous resin films) yielded unacceptable levels of porosity (3–8%). Tavares [10] measured the through-thickness air permeability of a commercial semi-preg ('Zpreg') and an equivalent unidirectional (UD) prepreg constructed with continuous resin. The permeability of the semi-preg material was three orders of magnitude greater than that of the continuous film prepreg before and during the cure cycle, a result attributed to a network of dry interconnected pore spaces in the semi-preg design. As these studies demonstrate, prepregs featuring discontinuous resin films increase the capacity for air evacuation in the *z*-direction (transverse) by creating efficient egress pathways. This effect is attributed to the much shorter air evacuation distances in the through-thickness direction (on the order of millimeters) as compared to the in-plane direction (on the order of meters). Discontinuous resin not only increases the efficiency of air evacuation but also entraps less air between plies. VBO prepregs with discontinuous resin have the potential to mitigate process-induced defects and impart robustness to the manufacture of aerospace composites *via* OoA methods.

Semi-pregs can be produced by different methods. We have previously reported one such method, which yields finely tuned resin distribution patterns and high through-thickness permeable prepregs [11–13]. The method relies on polymer film dewetting on a low surface energy substrate [14]. Using this method, resin film is first perforated on a silicone-coated backing paper (substrate) to create an array of nucleation sites. The film is then heated, causing resin to recede from the nucleation sites. The resin recession is driven by the surface tension between the low surface energy substrate (the silicone-coated backing paper) and the resin [14–17]. The dewetted resin is transferred onto a fiber bed by briefly pressing the constituents in a hydraulic press. This technique can be used to create a variety of resin patterns, including stripes, islands, and grids. In addition, the resin patterns created with this technique can in principle be applied to any dry fiber bed.

Objectives. The goal of this study is to assess the design and application of the semi-preg format in various common but challenging manufacturing conditions. Previous work has demonstrated the benefits of discontinuous resin application in prepreg processing. What has yet to be developed is a broad range of product forms for semi-pregs. The key developments described in this work are: (1) the fabrication of semi-preg produced from fiber beds with various fiber types, weave types, and areal weights, and (2) the production of complex parts using a woven semi-preg format. In this context, design considerations and limitations of semi-preg fabrication are also discussed.

Results reveal that low porosity laminates can be fabricated using semi-pregs with various woven fiber bed architectures. The use of discontinuous resin increases overall resin thickness, which slightly increases the bulk factor. To address concerns regarding the increase in bulk factor, curved laminates with concave and convex corners were produced. Ultimately, part quality did not decrease with the use of semi-pregs in the production of complex shapes. Finally, initial design guidelines are offered that outline the dimensional limitations of resin patterns, degree-of-impregnation (DOI) of semi-preg, placement of constituents considering the general direction of the fiber bed and the resin pattern, and the use of the polymer film dewetting technique on some of the most widely used resin systems. This work provides the first guidelines for the design of semi-pregs – an important modification of OoA prepreg format that has the potential to enhance the robustness of VBO processing of prepreg laminates.

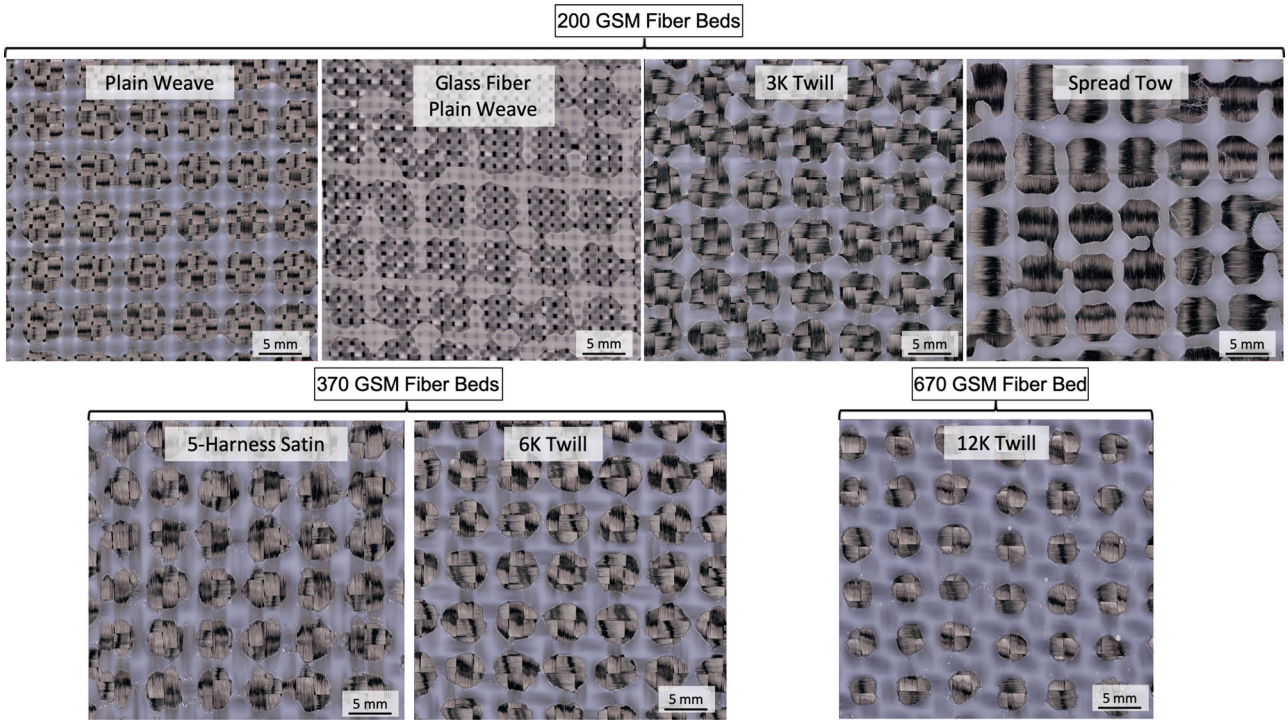

Figure 1. Semi-pregs prior to cure, showing discontinuous resin distribution (fabricated *via* polymer film dewetting) on each of the fiber bed types evaluated.emi-pregs

2. Materials and methods

Prepreg fabrication. A total of seven fiber beds were evaluated. Three fiber areal weights (200, 370, and 670 GSM) were selected. Unless otherwise noted, fabrics were carbon fiber. At 200 GSM, four fabric types were evaluated: plain weave, glass fiber plain weave (Fibre Glast Development Corporation, Ohio, USA), 3 K twill (Fibre Glast), and spread tow (Textreme, Sweden). The production of spread tow fiber beds involves the spreading of a tow into a thin and flat UD tape and then weaving into a fabric. For 370 GSM, a 5-harness satin (Fibre Glast) and a 6 K twill (Fibre Glast) fiber bed were evaluated. Finally, at 670 GSM, a 12 K twill fiber bed (Fibre Glast) was evaluated. A twill weave was selected for each areal weight to enable direct comparisons. The designations 3 K, 6 K and 12 K refer to the numbers of fibers within each tow (i.e. 3000, 6000 or 12,000 fibers per tow).

Semi-preg and conventional prepreg plies were fabricated with epoxy resin (PMT-F4, Patz Materials & Technology, California, USA) at a resin content of 35–36%. Semi-pregs were produced *via* selective dewetting of resin film [11, 12]. With the neat resin film on the silicone-coated backing paper (a low surface energy substrate), nucleation sites were introduced using either a hand-held spike roller (HR-2, Robert A. Main & Sons, Inc., New Jersey, USA) or a box cutter. The spike roller pins were spaced at 6.35 mm, and the roller was passed over the entire film in straight passes. Using a box cutter, the resin on the silicone-coated backing paper was scored in straight passes. The resin film was then placed in an air-circulating oven (Blue M Oven, Thermal Product Solutions, Pennsylvania, USA) to dewet and grow the openings at the nucleation sites. The resin film was heated for 2 min at 104 °C. Subsequently, the resin film was attached to the fiber beds by pressing the constituents briefly in an unheated hydraulic press (G30H-18-BCX, Wabash MPI, Indiana, USA). Images of discontinuous resin patterns produced using a spike roller, after application to various fiber beds, are presented in Figure 1.

To produce flat laminates, 16 plies of prepreg were stacked in a $[0/90]_{4s}$ sequence, where applicable. Initially, each ply was cut to 150 mm × 150 mm, and after stacking, the edges of the stack were trimmed, resulting in dimensions of 140 mm × 140 mm. The laminates were vacuum bagged using standard consumables. Rather than utilizing edge breathing (common practice with commercial VBO prepregs), the perimeter of each laminate was sealed with vacuum tape to restrict air evacuation solely to the through-thickness direction. Sealed edges were used to approximate process conditions that limit or prevent in-plane air evacuation (e.g. large or complex parts, parts with ply drops or corners). Laminates were cured according to the recommended cure cycle: a ramp of 1.5 °C per min to 121 °C followed by a 2-h dwell.

Commercial prepregs are produced from various resin systems, including cyanate ester and bismaleimide (BMI). To assess the compatibility of semi-preg fabrication *via* resin dewetting with different resin systems, the technique was employed using a

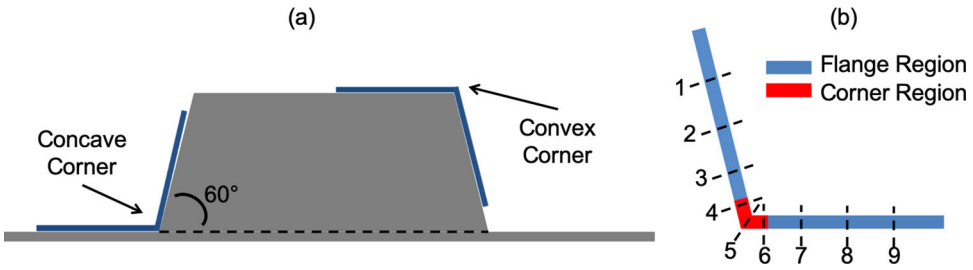

Figure 2. (a) A custom test fixture, which allowed simultaneous production of a 60° concave and a 60° convex corner laminate (with a rounded radius of 9.5 mm). (b) Locations of measurement along the flanges and corners to calculate the coefficient of variation (CoV).

cyanate ester resin film (54 GSM, PMT-F27, Patz Materials & Technology, California, USA), a BMI resin film (71.5 GSM, RS-8HT, Toray, California, USA), and a toughened epoxy resin film (71.5 GSM, CYCOM 5320-1, Solvay, USA).

Porosity measurements. To evaluate the surface porosity of cured laminates, images of regions 38 mm × 38 mm were recorded using a digital microscope (VHX-5000, Keyence Corporation of America, California, USA). These images were recorded at three locations across the laminate surface. For bulk void content, mutually orthogonal sections were prepared from the center of each laminate. Cross-sections were polished, and regions 5 mm × 20 mm were imaged.

Images were analyzed using software (ImageJ) to determine void contents. A series of steps was performed manually to produce binary porosity images. Using the software, images were converted to black pixels for voids and white pixels for the rest of the laminate. The percent porosity was calculated from the number of black and white pixels:

$$Porosity\ (\%) = \frac{p_{black}}{p_{white} + p_{black}} \times 100\ \% \qquad (1)$$

where p is the number of pixels.

Bulk factor. Bulk factor is defined as the ratio of the initial thickness, t_i, of the prepreg stack (prior to cure) to the final thickness, t_f, of the laminate (after cure):

$$Bulk\ Factor\ = \frac{t_i}{t_f} \qquad (2)$$

To calculate the bulk factor, the thickness of a laminate was measured prior to cure using a caliper at four locations around the perimeter. After cure, the laminate was sectioned, and a caliper was used to measure the thickness of the laminate at four locations throughout the cross-section.

Complex shapes. To fabricate curved laminates, a custom test fixture [18] was utilized, featuring a 60° concave and a 60° convex corner (with a rounded radius of 9.5 mm), yielding parts with common geometric complexities (Figure 2a). Tooling was machined from a single billet of aluminum to avoid leaks, and tool surfaces were fine polished. 8-ply laminates with dimensions of 75 mm × 130 mm were produced using a 370 GSM 5-harness satin fiber bed.

An accepted metric for corner quality is thickness variability between the flanges and the curved portion. Parts produced at a concave corner are expected to have corner thickening from pooling of resin. On the other hand, parts made at a convex corner are expected to have corner thinning. To determine the thickness variability, nine locations were measured at the flanges and corner, as illustrated in Figure 2b. The average thickness, $\bar{x}$, was calculated using the following equation:

$$\overline{x} = \frac{\sum x_i}{n} \qquad (3)$$

where x_i is the thickness at each individual location and n is the number of measurement locations. The coefficient of variation (CoV) was then calculated using the following equation:

$$Coefficent\ of\ Variation\ (CoV) = \frac{1}{\overline{x}}\sqrt{\frac{\sum (x-\overline{x})^2}{(n-1)}} \qquad (4)$$

where the variables are defined identically as the previous equation.

In situ monitoring. To monitor the resin flow front during processing, the surfaces of the semi-pregs were tracked *in situ* using the technique described by Hu *et al.* [19, 20]. Four-ply semi-preg stacks using a 5-harness satin fiber bed were fabricated using either a grid or a striped pattern. The stacks were laid against a glass window of an oven and vacuum-bagged with standard consumables, sealing edges to prevent gas egress. Resin flow was monitored and recorded during a standard cure cycle using a digital microscope and time-lapse video acquisition (Dino-Lite US, Dunwell Tech, Torrance, CA, USA). Temperature was monitored

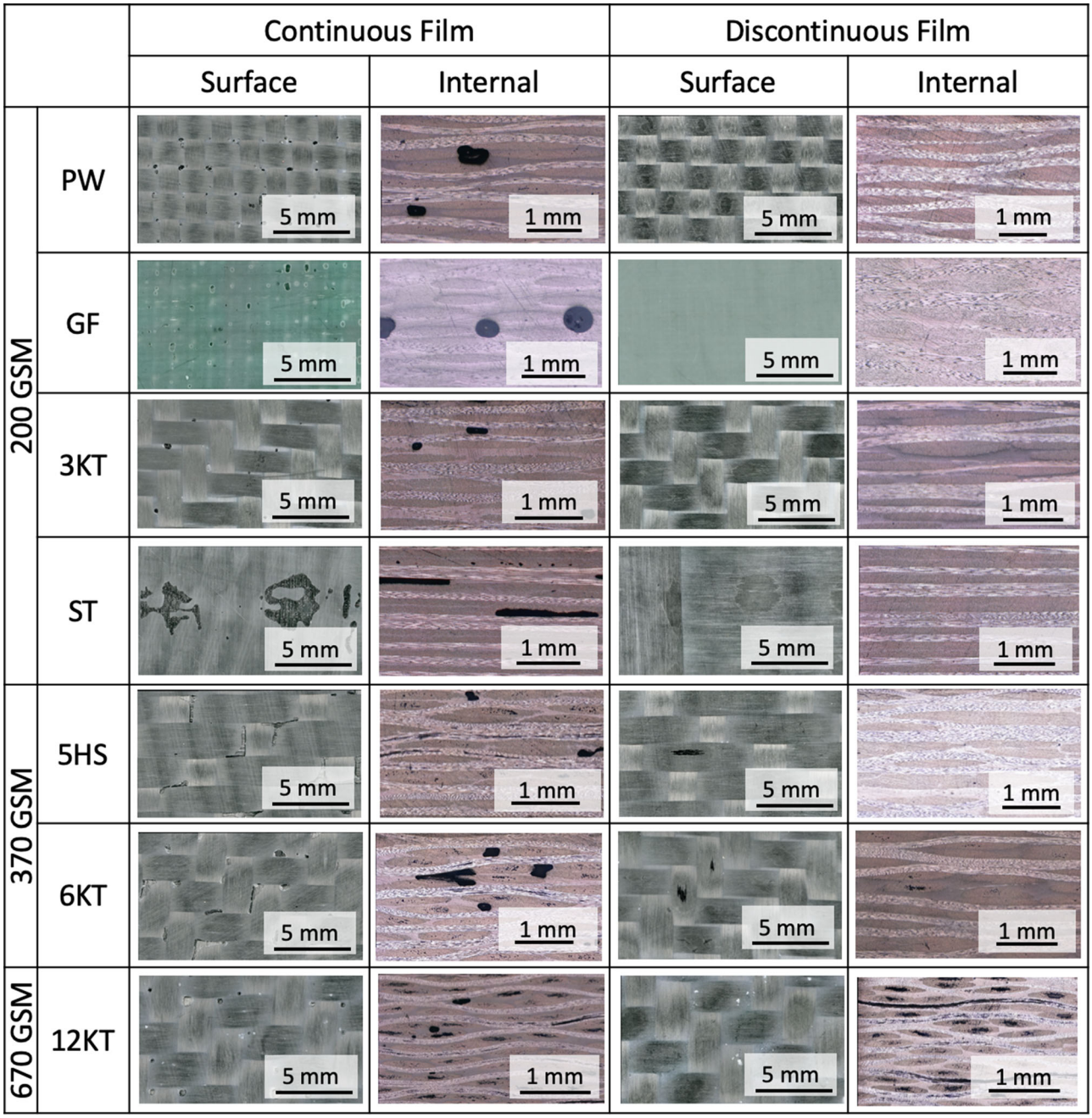

Figure 3. Surfaces and cross-sections of each of the semi-preg formats evaluated. The fiber bed types are indicated as: PW (plain weave), GF (glass fiber plain weave), 3KT (3 K twill), ST (spread tow), 5HS (5-harness satin), 6KT (6 K twill), and 12KT (12 K twill).

with a USB thermocouple data logger (Lascar Electronics EasyLog EL-USB-TC-LCD), which was attached adjacent to the laminate and directly on the glass tool plate.

3. Results

3.1. Quality analysis of semi-preg formats

Key differences exist between UD and woven fiber beds. Woven fabric exhibits crimp, or fiber waviness, whereas crimp in UD fiber beds is negligible. Crimp varies based on weave type and can range from minimal (i.e. spread tow) to large (i.e. plain weave). High crimp generally reduces laminate strength [21]. Secondly, woven fiber beds contain pinhole openings between crossing tows, which enhance transverse air evacuation, while UD fiber beds do not. Finally, flow of resin in a woven fiber bed is multidimensional. Resin flows more rapidly through pinholes and in the depressions at tow intersections. Resin therefore flows through pinholes and depressions (macroflow) before saturating tows (microflow). This dual-scale flow does not occur in UD fiber beds. These differences are expected to affect both gas and resin flow in semi-preg materials.

Both conventional prepregs and semi-pregs were fabricated with a variety of fiber types, weave types,

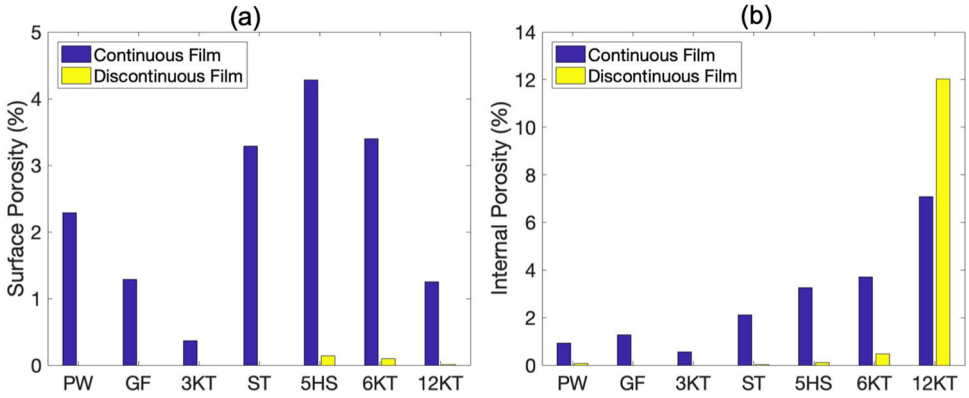

Figure 4. (a) Surface porosity and (b) internal porosity of each of the prepreg and semi-preg formats evaluated. The fiber bed types are indicated as in Figure 3.

and fiber bed areal weights, after which cured laminate quality was assessed. As described in Section 2, laminates were fabricated from three areal weights (200, 370, and 670 GSM), four weave types (plain weave, twill, satin weave, and spread tow), and two fiber types (carbon and glass fibers). Micrographs of surface and internal porosity of all samples are presented in Figure 3, with the seven fiber bed types indicated as PW (plain weave), GF (glass fiber plain weave), 3KT (3 K twill), ST (spread tow), 5HS (5-harness satin), 6KT (6 K twill), and 12KT (12 K twill).

The first and second columns of Figure 3 depict the surface and internal porosity, respectively, of laminates produced with conventional OoA prepreg formats (continuous film) using the seven different fiber beds. All seven conventional laminates exhibited high levels of surface and internal porosity, both of which were apparent *via* visual inspection. In all seven conventional laminates, porosity was concentrated at locations corresponding to fabric pinholes and the depressions at tow intersections. During cure, these features create points of low pressure toward which resin and air migrate. Specifically, in the conventional spread tow laminate (fourth row, first and second columns), in addition to porosity at the pinholes and depressions, intra-tow porosity was also observed due to the flatness of this fabric. In these prepregs produced with spread tow fabric, the surface porosity observed resembled defects observed with UD fiber beds, as shown in previous work [11, 12].

The third and fourth columns of Figure 3 depict the surface and internal porosity, respectively, of laminates produced with semi-preg using the seven different fiber beds. Each of the four semi-preg laminates fabricated with 200 GSM fiber beds displayed near-zero surface and internal porosity, as depicted in the first through fourth rows of the third and fourth columns. Notably, in the laminate made from spread tow semi-preg (fourth row, third column), surface porosity was not detected, but vestiges of the applied discontinuous resin pattern were observed on the cured part surface. Similar surface features have been reported in previous studies of semi-preg materials made from UD fiber beds [11, 12]. Semi-preg laminates produced with 370 and 670 GSM fiber beds exhibited both surface and internal porosity after curing, as depicted in the fifth through seventh rows of the third through fourth columns. The surface and internal porosity was attributed to incomplete saturation of the fiber bed during cure, indicating that resin flow distances were too long to fully infiltrate. This intra-tow (flow-induced) porosity was greater for 670 GSM than for 370 GSM fabrics, indicating a potential upper limit on fabric thickness for the present format of semi-preg processing. No inter-ply porosity (gas induced) was observed in any semi-preg samples.

A graphic summary of the surface and internal porosity for all samples is shown in Figure 4, with the fiber bed types indicated as in Figure 3. The surface porosity (Figure 4a) of all conventional prepreg samples was greater than 1%, except for the 3 K twill sample at 0.4%. All semi-preg samples, in contrast, exhibited less than 1% surface porosity, with most samples displaying no surface voids. While surface porosity was visible for the fiber beds with larger areal weights ($\geq$370 GSM), the measured surface porosity was $\sim$0.1%. Internal porosity (Figure 4b) for all samples produced using prepreg with continuous film was 1% or more, with porosity levels increasing with fiber areal weight. Except for the panel produced with 12 K twill, the semi-preg samples showed less than 1% porosity. Interestingly, the 12 K twill laminate produced from semi-preg resulted in more porosity (12.0%) than the sample fabricated from prepreg with continuous resin (7.1%). These findings indicate that an upper limit on fabric weight may exist for successful semi-preg processing, or that the cure process or semi-preg format might require modification.

The potential benefits of semi-preg materials have been previously reported, but a versatile range of product forms has not been developed. Here, we

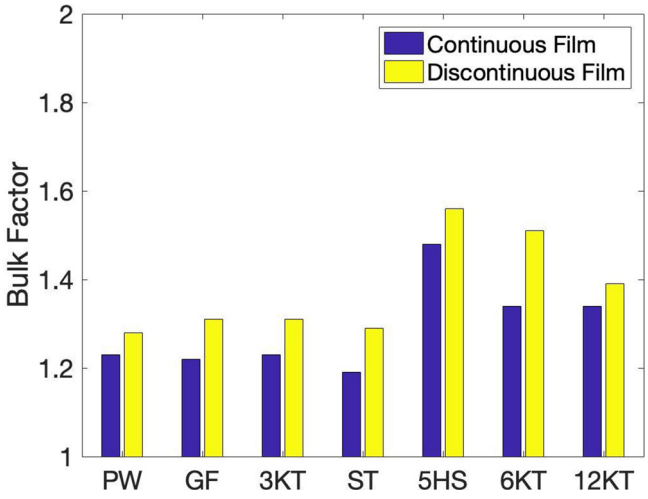

Figure 5. The measured bulk factor of each of the prepreg and semi-preg formats evaluated.

have demonstrated that semi-preg can be fabricated from a range of fiber types, weave types, and fiber bed areal weights. The laminates produced from semi-preg with low and intermediate areal weight fabrics showed lower porosity (< 1%) than comparable laminates produced with conventional format prepreg. However, in laminates produced from high areal weight fabrics, porosity increased markedly (12.0%), because fiber bundles were too thick to fully impregnate during cure. To resolve this issue, further work must be undertaken, such as employing a higher degree of impregnation (DOI) to reduce the flow distance (which will be discussed in Section 3.4) or utilizing a tailored resin system with longer flow times at low viscosity.

3.2. Bulk factor

Bulk factor also was calculated for each laminate described in Section 3.1. Bulk factor is relevant for fabrication of contoured parts because a large bulk factor can cause wrinkling and/or bridging of plies. In principle, a bulk factor of 1.0 represents no change in thickness during cure, a characteristic generally preferred. However, prepregs that incorporate dry regions for air evacuation intrinsically possess bulk factors > 1. Bulk factor is further increased when discontinuous resin distributions are used [11, 12].

For the semi-preg and prepreg formats evaluated (Figure 5), bulk factors varied with weave type because of the inherent differences in fiber bed characteristics (i.e. crimp). In addition, the bulk factor generally increased as areal weight increased. The average difference in bulk factor between conventional prepreg and semi-preg with the same fiber type was ~0.1. The fiber bed architecture that produced the largest overall bulk factor was 5-harness satin (5HS). This fiber bed was selected for further study *via* fabrication of panels with concave and convex corner geometries (discussed in Section 3.3).

3.3. Complex shapes

Laminates with complex geometries were evaluated to determine if and how the bulk factor increase associated with a semi-preg design affected part quality. Laminates with concave and convex corners were cured using both semi-pregs and conventional format prepregs, for a total of four curved laminates. Prepregs with a higher bulk factor undergo greater compaction during cure and often will not conform readily to a curved surface. When the bulk factor is high, prepreg and consumable materials can bridge over concave molds or wrinkle over convex tooling [22–29], introducing in-plane stresses and reducing the compaction pressure at corners.

Images of the four sample cross-sections are presented in Figure 6. As the four images show, neither the semi-preg nor the conventional format prepreg produced wrinkling or extensive bridging at laminate corners. However, a key distinction between the two prepreg formats was the levels of porosity in the cured laminates. The conventional prepreg sample exhibited both intra-tow and inter-ply porosity, as shown in the first column. In contrast, the semi-preg sample exhibited negligible intra-tow porosity, as shown in the second column. These results were consistent with those discussed in Section 3.1.

The CoV (Equation (4)) is a metric of corner part quality which describes the variability in thickness between the flanges and the curved surface of a complex part. The calculated CoV of both convex and concave corners made with conventional prepreg was 0.08. For the corners made with semi-preg, the CoV was 0.09, indicating that discontinuous film may slightly increase the variability in corner thickness. This increase can be attributed to either inherent

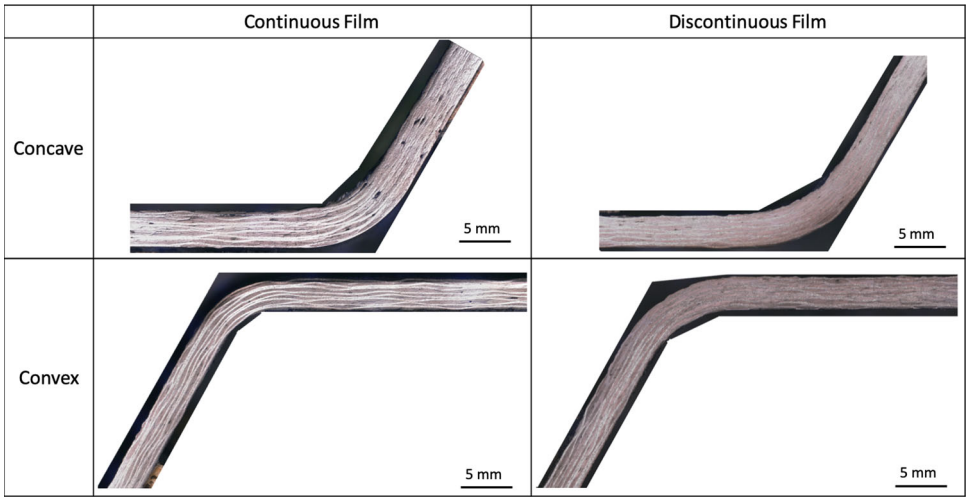

Figure 6. Part quality obtained from processing 5-harness satin prepregs and semi-pregs at a concave and convex corner.

experimental variation or to the higher bulk factor of the semi-preg.

3.4. Design considerations & limitations for semi-preg fabrication

Design considerations and limitations for the fabrication of semi-pregs were explored in the context of processing. Certain aspects of design and fabrication of semi-pregs are critical to achieving high-quality parts *via* OoA/VBO processing. Here, we examine: (1) dimensional limitations of the discontinuous pattern due to resin thickness and to uniformity; (2) DOI of the resin in the fiber bed; (3) placement of discontinuous patterns and fiber beds that are either isotropic or anisotropic; and (4) polymer film dewetting of different resin systems.

Feature dimensions. Polymer film dewetting typically occurs at the edge of a dry region (i.e. perforations, tears, or deep depressions). When producing resin patterns for semi-preg by dewetting, nucleation sites are introduced by scoring or piercing the resin where openings are desired. However, a regular pattern is more difficult to achieve with resin that is nonuniform (high discontinuity), because unintentional nucleation sites will exist. Nonuniformity in resin films typically consists of uneven thickness, gaps, and dry space, which often arises during filming. These defects are more prevalent in thinner resin films and have a greater effect.

Examples of striped resin patterns with different spacings of imposed nucleation sites are presented in Figure 7. The first row depicts the resulting discontinuous resin patterns at 26 GSM when scored at 5-mm and 1-mm intervals. As shown in the left micrograph, the resin did not dewet uniformly when scored at 5 mm, and dewetting nucleated spontaneously between the scorings. As depicted in the right micrograph, the resulting pattern became more uniform when the scoring was reduced to 1-mm intervals, although some dewetting still occurred along the resin stripes.

The second row depicts the resulting discontinuous resin patterns at 54 GSM when scored at 10-mm and 5-mm intervals. As shown in the right micrograph, by doubling the resin areal weight from 26 GSM to 54 GSM, uniform stripes were achieved with dewetting after scoring at 5-mm intervals. However, as depicted in the left micrograph, when scoring spacing was increased to 10 mm, feature precision was lost, and resin stripes were irregular in shape. The third row depicts a resulting discontinuous resin pattern at 188 GSM. Here, the patterning was uniform, even with scoring at 20-mm intervals.

Uniform patterns can be achieved with thin resin films if nucleation sites are closely spaced. However, uniform patterns are difficult to achieve for thin and nonuniform resin films when nucleation sites are spaced further apart, as depicted in the left micrographs of the first and second rows of Figure 7. On the other hand, uniform patterns are readily achieved with thick resin films, as shown in the third row. To achieve uniform patterns across all resin thicknesses, the resin filming process must be carefully controlled to restrict random dewetting.

Degree of impregnation. The method described for fabricating semi-pregs *via* polymer film dewetting results in a DOI near zero. Low DOI values require transverse microflow to saturate fiber tows prior to gelation. Results in Section 3.1 revealed that low porosity laminates were not achieved when semi-preg was fabricated with the thickest fiber bed (12 K, 670 GSM). Presumably, the porosity resulted from the longer flow distances required, which

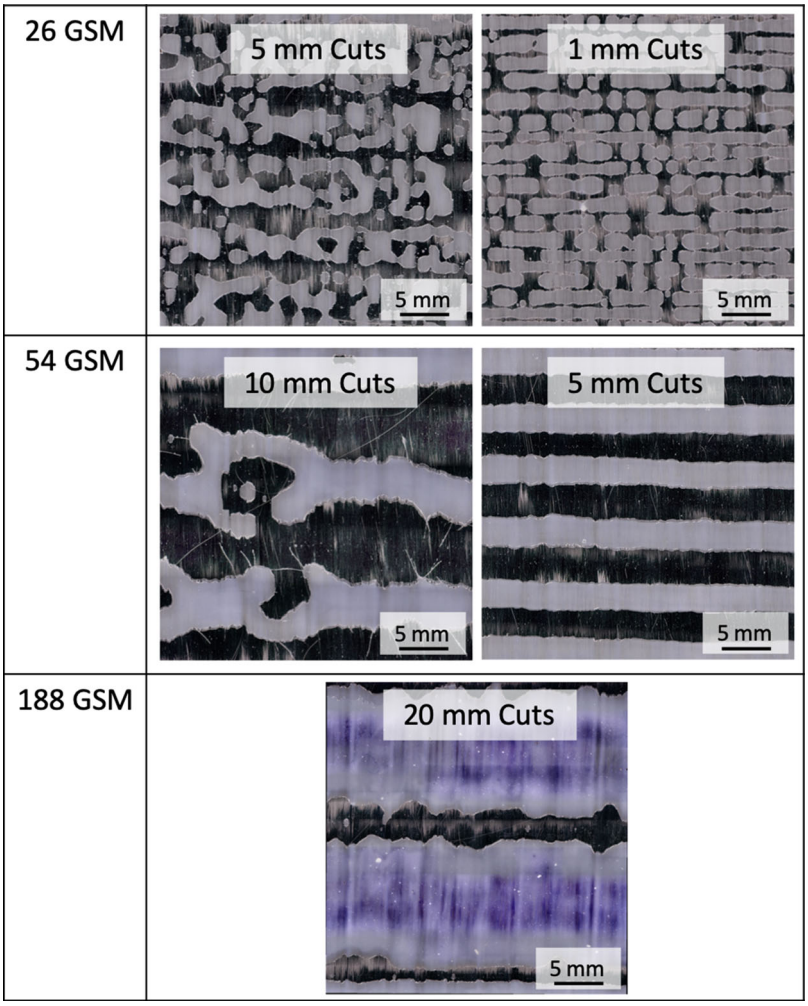

Figure 7. Resin with various areal weights that were cut at different distances to demonstrate the limitations of feature dimensions for uniform patterning.

prevented full saturation of fiber tows. One approach to this problem is to increase the DOI to reduce the flow distances required to achieve saturation during cure. However, attempts to increase DOI can potentially eliminate resin discontinuities and compromise the semi-preg format, as described below.

The original intention of creating conventional OoA prepregs with partial DOI (versus full saturation of the fiber bed) was to retain dry space at the center of fiber tows, which was a technological advancement in prepreg manufacturing [30]. In conventional OoA prepregs, these in-plane dry regions allow air to evacuate the prepreg *via* edge breathing. DOI is defined as:

$$Degree\ of\ Impregnation\ (DOI) = 1 - \frac{A_{dry}}{A_{tow}} \quad (5)$$

where A_{dry} is the dry tow area and A_{tow} is the entire tow area (dry and saturated) [31]. Commercial OoA prepregs exhibit levels of DOI which range from 0.05 to 0.5. However, the prepreg fabrication method presented here involves briefly pressing fibers and resin films (continuous or discontinuous) using an unheated hydraulic press. This method results in a negligible DOI into the fiber bed, and the resin adheres only to the outer fibers of tows.

Images of the DOI of the resin into a 5-harness satin fiber bed produced in this manner is presented in Figure 8(a,b). The micrograph of the surface is depicted in Figure 8(a), and the micrograph of the cross-section is depicted in Figure 8(b). The cross-sectional image (Figure 8(b)) shows, in addition to exhibiting near-zero DOI, extensive macroflow between tows, as well as entrapped air bubbles. A larger DOI would reduce the resin flow distances required, as well as the bulk factor. Increasing the DOI was attempted by applying a pressure of 0.09 MPa to the semi-preg at 50 °C for 15 min using a hydraulic press. Images of the surface and cross-section of the semi-preg after this treatment are displayed in Figure 8(c,d). This treatment altered and disrupted the discontinuous resin pattern, as illustrated by comparing Figure 8(a) and 8(c). When pressure and temperature were applied, resin flowed preferentially along the length of the fibers before infiltrating the fiber tows. In Figure 8(d), an example of an entire tow bundle is outlined in purple, and the remaining dry fiber region is outlined

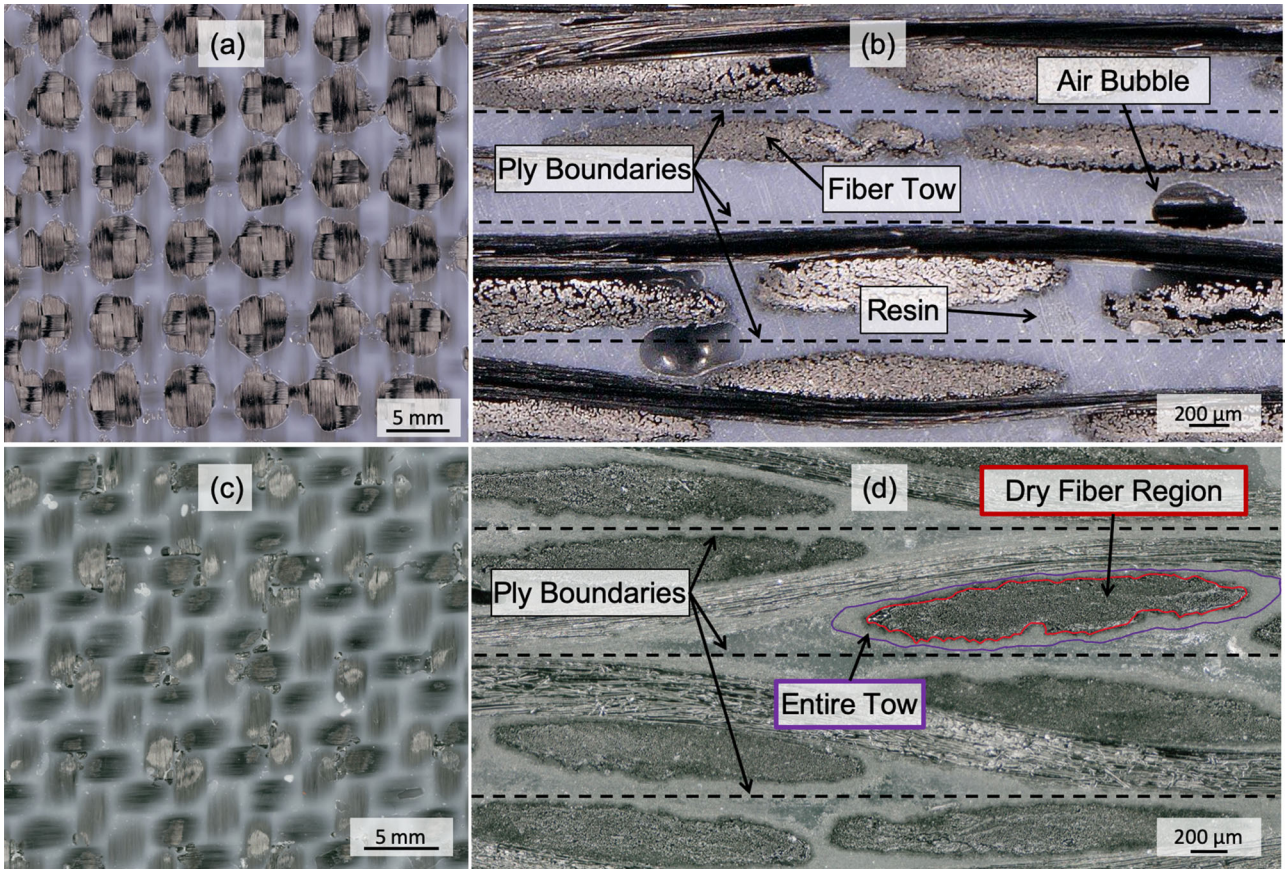

Figure 8. (a) The surface of semi-preg with a DOI of zero. (b) The cross-section of a semi-preg with a DOI of zero. (c) Surface of semi-preg that underwent elevated temperature and pressure to increase the DOI. (d) Cross-section of semi-preg with an increased DOI.

in red. Using Equation (5), the volumes of these two outlined regions were used to calculate the DOI. Here, the DOI increased to 0.25 +/− 0.10.

A negligible DOI in semi-preg materials with thick fiber beds inevitably will result in long flow distances. However, conventional means of increasing the DOI (i.e. high temperature and applied pressure) alter discontinuous resin patterns. Further development in prepreg production methods will be required to achieve semi-pregs with controlled resin patterning and increased DOI (and reduced bulk factors).

Isotropy & anisotropy. Some fiber beds (i.e. UD) and some discontinuous resin patterns (i.e. stripes) are anisotropic. Other fiber beds (i.e. satin weaves) are not anisotropic, but have adjacent, unidirectionally aligned segments of tows (AUDAST). An example of an AUDAST fiber bed is 5-harness satin fabric. On one side of this fabric, segments of adjacent tows are aligned globally in one direction. On the obverse side, segments of adjacent tows are also aligned globally in one direction, but perpendicular to the segments of the first side. The segments on each side of the fabric are woven together, which results in each side of the fabric containing perpendicular tow warps. Thus, the fabric surface is not entirely isotropic. This locally anisotropic structure of the AUDAST fabric surface affects resin flow in semi-pregs, particularly during initial stages, and can potentially disrupt, distort, and even eliminate patterns of discontinuous resin.

When imposing resin patterns on such fiber beds (anisotropic and AUDAST), the placement of the resin pattern in relation to the fiber orientation at the fabric surface can affect the ability to saturate the fiber bed. During cure, resin flow occurs preferentially along fiber directions, rather than transversely [11, 12, 32]. Thus, if an anisotropic resin pattern is placed parallel to an anisotropic or AUDAST fiber bed (e.g. striped resin pattern on 5-harness satin fiber bed), fiber bed saturation may not be achieved. Such care need not be required with isotropic fabrics (i.e. plain, twill weaves) and/or an isotropic resin patterns (i.e. uniform grid, islands).

To determine the influence of resin pattern anisotropy and fiber orientation on fiber bed impregnation, *in situ* observations were performed using a transparent tool plate [19, 20]. A typical cure cycle was employed using vacuum bagged semi-pregs with select resin distributions applied to a 5-harness satin fiber bed. Figure 9 shows the

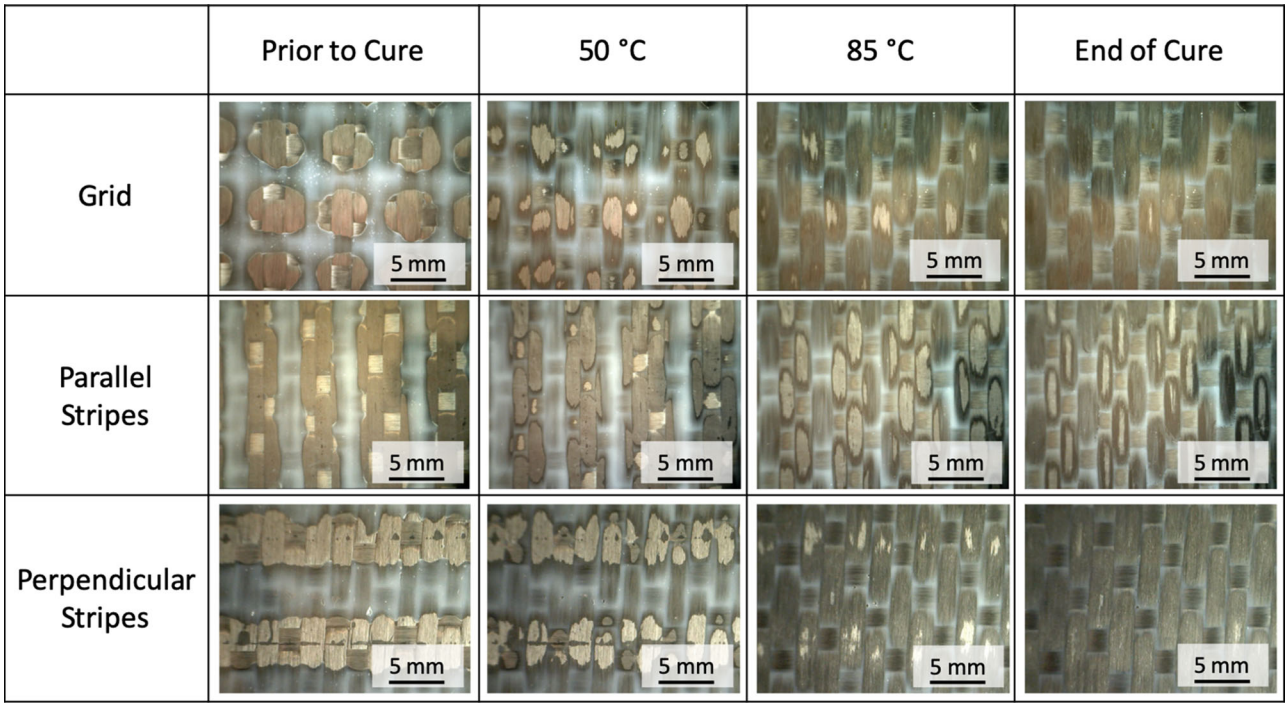

Figure 9. Resin flow for various pattern types and pattern placement with respect to the fiber bed during the cure cycle.

progression of resin flow at the tool/part interface at different temperatures during the cure of each of the semi-preg formats analyzed.

The first row of Figure 9 depicts the flow of resin during the cure cycle of a 5-harness satin semi-preg with an isotropic grid pattern. Resin quickly filled pinholes and depressions created by tow crimp of the 5-harness satin fabric (macroflow), as shown in the 50 °C micrograph. Subsequently, micropore spaces within the fiber tow bundles were slowly filled by microflow, as shown in the 85 °C micrograph. By the end of the cure cycle, the fiber bed was saturated, and exhibited only minor surface porosity, as shown in the 'End of Cure' micrograph.

The second row of Figure 9 depicts the flow of resin during the cure cycle of a 5-harness satin semi-preg with an anisotropic striped pattern applied parallel to the primary fiber direction. Resin initially filled adjacent pinholes and the depressions of adjacent tows, as shown in the 50 °C micrograph. Thereafter, resin flowed preferentially into fiber tows that were perpendicular to the resin stripes, as shown in the 85 °C micrograph. This process was much slower than the infiltration times required for the grid pattern and resulted in regions of dry fiber tows (~9.2% of the entire surface area). The third row of Figure 9 depicts the flow of resin during the cure cycle of a 5-harness satin semi-preg with an anisotropic striped pattern applied perpendicular to the primary fiber direction. Resin flow saturated this fiber bed much like the grid pattern depicted in the first row.

The results described above show that anisotropic resin patterns (e.g. stripes), when aligned parallel to an anisotropic or AUDAST fiber bed, yield only partial saturation. On the other hand, isotropic resin patterns, such as grids, are more robust and immune to adverse effects of fiber orientation. Thus, when designing semi-preg formats, isotropic patterns can be advantageous, as they effectively mitigate nonuniform flow issues and achieve full fiber bed saturation regardless of fiber orientation. Anisotropic patterns such as stripes must be intelligently applied to ensure proper placement with reference to the fiber orientation. However, stripes may be simpler and more convenient to produce relative to other pattern designs, such as islands or grid, depending on the production method of the discontinuous resin distribution [6, 7, 10].

Alternative resin systems. Prepregs are produced with a wide variety of thermoset resin types and formulations. To explore the versatility of semi-preg fabrication *via* polymer film dewetting, the technique was applied to select resin systems: cyanate ester, BMI, and a standard commercial OoA epoxy (CYCOM 5320-1, Solvay, USA).

Images of the discontinuous resin patterns pressed onto a UD carbon fiber bed and onto a plain weave glass fiber bed are shown in Figure 10. A grid pattern of cyanate ester was created and applied to glass fibers (cyanate ester is often reinforced with fibers other than carbon), as shown in

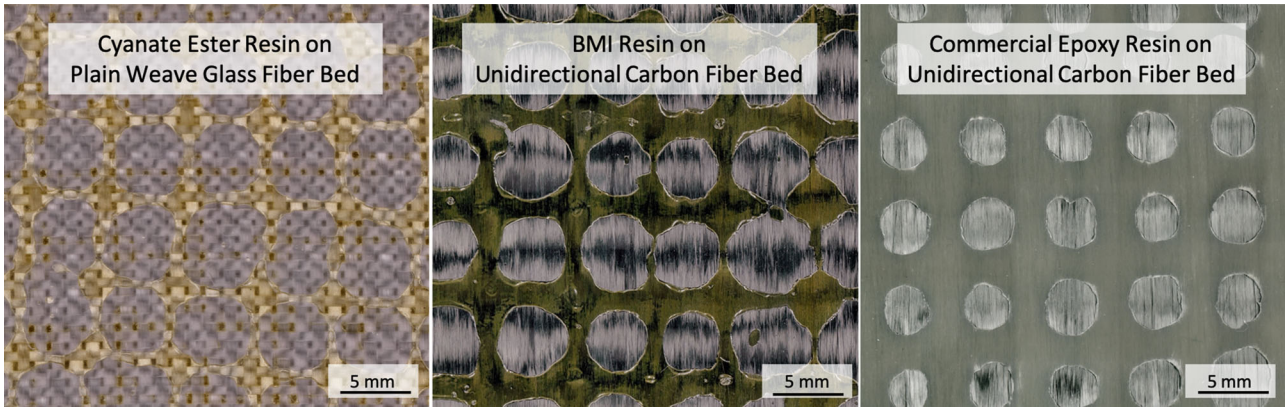

Figure 10. Bismaleimide (BMI), cyanate ester, and commercial epoxy (CYCOM 5320-1) films that were created into discontinuous distributions by initiating nucleation sites by a spike roller and subsequently heating the resins at 104 °C.

the left micrograph. Similarly, grid patterns of BMI resin and a commercial epoxy resin (CYCOM 5320-1) were created and applied to UD carbon fibers, as shown in center and right micrographs. To achieve the same feature dimensions as the epoxy resin patterns studied in previous sections, the cyanate ester and BMI resin were heated to 104 °C for only $10-15$ s. If heated for longer times, the resin film dewetted extensively, forming small droplets. However, achieving the same feature dimensions in the commercial epoxy required heating to 104 °C for more than 12 min. While a dewetting process can potentially be applied to any resin system, dewetting conditions require adaptation to the specific resin system and substrate. The BMI and cyanate ester films used here required less time ($10-15$ s) to achieve feature dimensions equivalent to the original epoxy resin system (2 min), a result of the higher interfacial tension with the silicone-coated backing paper. The commercial epoxy film had a lower interfacial tension with the backing paper and thus required more time ($>$ 12 min) to achieve similar dimensions.

The results shown in Figure 10 and described above demonstrate that polymer film dewetting can be used to produce discontinuous resin patterns from a range of resin systems. However, a resin can only be utilized for the fabrication of OoA parts if resin cure kinetics are amenable to low pressure processing [4]. VBO prepreg systems are designed to remain relatively viscous in the early stages of cure to limit infiltration, prevent resin bleed, and retain sufficient dry areas for air evacuation [2]. The overall viscosity profile, however, must also permit sufficient flow during the cure cycle to fully saturate the fiber bed [3]. The rheological evolution of VBO resins must, in essence, balance the need to prevent voids caused by entrapped gases (air and cure induced volatiles) as well as voids caused by insufficient flow. Provided these conditions can be met, a semi-preg fabricated with dewetted resin can be expected to consistently yield high quality laminates with OoA/VBO cure, even under adverse process conditions.

4. Conclusions

In general, laminates fabricated using semi-preg with a variety of fiber bed architectures exhibited near-zero porosity. In addition, semi-preg formats increased the bulk factor of VBO-fabricated laminates by ~0.1. Nevertheless, production of complex shapes using semi-preg revealed that part quality (i.e. wrinkling, bridging, and thickness variation) was similar to the quality achieved with conventional prepreg. By incorporating multiple design considerations, the dewetting technique was applied to other resin systems, such as cyanate ester and BMI, to create uniform and repeatable discontinuous resin patterns.

The use of semi-pregs to produce parts *via* VBO processing shows promise and may indeed impart robustness. Nevertheless, some key limitations of the approach were identified, and these may require further study. Current fabrication methods to create semi-pregs result in larger bulk factors than conventional OoA prepregs ($\Delta\sim0.1$), due primarily to the near-zero DOI, and secondarily to thicker resin from the dewetting process. In addition to longer flow distances, the low DOI will limit the ability to rework plies (lift and reposition) when required. Only practical experience will determine how serious these drawbacks will be [33]. However, the advantages imparted by the short breathe-out distances in semi-pregs (enhancing robustness to the VBO manufacturing process) are expected to outweigh these drawbacks. In particular, the use of semi-pregs may help to restore the process robustness sacrificed by abandoning autoclave curing for OoA processing. Nonetheless, one crucial challenge that remains is to demonstrate the scalability of the dewetting process. Current work has demonstrated only a lab-scale batch process and a continuous process has not yet been shown. However, the process

may in fact be backwards-compatible with hot-melt prepregging, since in principle, imprint/de-wet steps can be incorporated into existing prepreg production lines.

The development of semi-preg materials is a potential route toward robust OoA composite manufacturing. This work established that a large range of semi-preg product forms can be fabricated and manufactured into high-quality laminates for both flat and complex parts. The inherent manufacturing robustness imparted by the methods presented here can potentially expand the applicable uses of VBO prepregs within aerospace manufacturing and to other nonaerospace applications.

Acknowledgements

The authors are grateful to Claire Carlton for her assistance and for material donations from Airtech International (Cole Standish), Textreme (Jim Glaser), Toray Advanced Composites (Steve Smith), and Solvay.

Disclosure statement

No potential conflict of interest was reported by the authors.

Funding

This project was supported by the M.C. Gill Composites Center.

ORCID

Sarah G. K. Schechter http://orcid.org/0000-0001-9000-3093
Lessa K. Grunenfelder http://orcid.org/0000-0001-6561-401X
Steven R. Nutt http://orcid.org/0000-0001-9877-1978

References

[1] Hueber C, Horejsi K, Schledjewski R. Review of cost estimation: methods and models for aerospace composite manufacturing. Adv Manuf Polym Compos Sci. 2016;2:1–13.
[2] Ridgard C. Out of autoclave composite technology for aerospace, defense and space structures. Proceedings of the SAMPE 2009 Conference, Baltimore, MD; 2009.
[3] Steele M, Corden T, Gibbs A. The development of out-of-autoclave composite prepreg technology for aerospace applications. SAMPE Tech Conference, Long Beach, CA; 2001.
[4] Centea T, Grunenfelder LK, Nutt SR. A review of out-of-autoclave prepregs: material properties, process phenomena, and manufacturing considerations. Compos Part A Appl Sci Manuf. 2015;70:132–154.
[5] Pethrick RA. Bond inspection in composite structures. Compr. Compos. Mater. 2000;5:359–392.
[6] Roman M, Howard SJ. Boyd JD. Curable prepregs with surface openings. US patent 2014/0174641 A1, 2014.
[7] Grunenfelder LK, Dills A, Centea T, et al. Effect of prepreg format on defect control in out-of-autoclave processing. Compos Part A Appl Sci Manuf. 2017;93:88–99.
[8] Nutt S, Grunenfelder L, Centea T. High permeability composite prepreg constructions and methods for making the same. US patent PCT/US2018/012665, 2018.
[9] Grunenfelder LK, Katz S, Centea T, et al. Through-thickness permeable prepreg for robust vacuum bag only processing. SAMPE J. 2018.
[10] Tavares SS, Michaud V, Månson J. Assessment of semi-impregnated fabrics in honeycomb sandwich structures. Compos Part A Appl Sci Manuf. 2010;41:8–15.
[11] Schechter SGK, Centea T, Nutt SR. Polymer film dewetting for fabrication of out-of-autoclave prepreg with high through-thickness permeability. Compos Part A Appl Sci Manuf. 2018;114:86–96.
[12] Schechter SGK, Centea T, Nutt S. Fabrication of out-of-autoclave prepreg with high through- thickness permeability by polymer film dewetting. Sample Tech Conference, Long Beach, CA; 2018; p. 2018.
[13] Schechter SGK, Centea T, Nutt S. Effects of resin distribution patterns on through-thickness air removal in vacuum-bag-only prepregs. Compos Part A Appl Sci Manuf. 2020;130: 105723.
[14] Kohl JG, Singer IL. Pull-off behavior of epoxy bonded to silicone duplex coatings. Prog Org Coat. 1999;36:15–20.
[15] Kheshgi HS, Scriven LE. Dewetting: Nucleation and growth of dry regions. Chem Eng Sci. 1991;46:519–526.
[16] Roy S, Bandyopadhyay D, Karim A, et al. Interplay of substrate surface energy and nanoparticle concentration in suppressing polymer thin film dewetting. Macromolecules. 2015;48:373–382.
[17] Coussy O. Surface energy and capillarity. Mech. Phys. Porous Solids. Hoboken, NJ: John Wiley & Sons, Ltd; 2010. p. 107–147.
[18] Ma Y, Centea T, Nutt SR. Defect reduction strategies for the manufacture of contoured laminates using vacuum BAG-only prepregs. Polym Compos. 2017;38:2016–2025.
[19] Hu W, Grunenfelder LK, Nutt SR. In-situ observation of void transport during vacuum bag-only cure. SAMPE Tech Conference, Long Beach, CA; 2016.
[20] Hu W, Grunenfelder LK, Centea T, et al. In-situ monitoring of void evolution in unidirectional prepreg. J Compos Mater. 2017;52:2847–2858.
[21] Hörrmann S, Adumitroaie A, Viechtbauer C, et al. The effect of fiber waviness on the fatigue life of CFRP materials. Int J Fatigue. 2016;90:139–147.
[22] Albert C, Fernlund G. Spring-in and warpage of angled composite laminates. Compos Sci Technol. 2002;62:1895–1912.
[23] Hoa SV. Factors affecting the properties of composites made by 4D printing (moldless composites manufacturing). Adv Manuf Polym Compos Sci. 2017;3:101–109.
[24] Kar KK, Sharma SD, Mohanty A, et al. Short-term effect of distilled water, seawater and temperature

on the crushed and interlaminar shear strength of fiber reinforced plastic composites made by the newly proposed rubber pressure molding technique. Polym Compos. 2008;37:915–924.

[25] Kar KK, Sharma SD, Kumar P. Effect of rubber hardness on the properties of fiber reinforced plastic composites made by the newly proposed rubber pressure molding technique. Polym Compos. 2007; 37:915–924.

[26] Kar KK, Sharma SD, Sah TK, et al. Development of rubber pressure molding technique using butyl rubber to fabricate fiber reinforced plastic components based on glass fiber and polyester resin. J Reinf Plast Compos. 2007;26:269–283.

[27] Kar KK, Sharma SD, Behera SK, et al. Development of rubber pressure molding technique using silicone rubber to fabricate fiber-reinforced plastic components based on glass fiber and epoxy resin. J Elastom Plast. 2007;39:117–131.

[28] Kar KK, Sharma SD, Behera SK, et al. Development of rubber pressure molding technique using butyl rubber to fabricate fiber reinforced plastic components based on glass fiber and epoxy resin. J Appl Polym Sci. 2006;101: 1095–1102.

[29] Kar KK, Sharma SD, Kumar P, et al. Pressure distribution analysis of fiber reinforced plastic components made by rubber pressure moulding technique. J Appl Polym Sci. 2007;105:3333–3354.

[30] Repecka L, Boyd J. Vacuum-bag-only-curable prepregs that produce void-free parts. SAMPE Tech Conference, Long Beach, CA; 2002.

[31] Palardy-Sim M, Hubert P. Characterization of the degree of impregnation of out-of-autoclave prepreg. 20th International Conference on Composite Materials, Copenhagen, July 19–24th 2015.

[32] Martinez P, Jin B, Nutt S. Effect of fiber bed architecture on single resin droplet spread for prepreg manufacturing. CAMx Conference Proceedings, Anaheim, CA; 2019.

[33] Elkington M, Bloom D, Ward C, et al. Hand layup: understanding the manual process. Adv Manuf Polym Compos Sci. 2015;1:138–151.